Supporting Online Material

Adaptive evolution of an sRNA that controls *Myxococcus* development

Yuen-Tsu N. Yu, Xi Yuan and Gregory J. Velicer

Online Abstract

Small RNA (sRNA) molecules regulate a vast array of processes in biology, but evidence for adaptive evolution of sRNA sequences has been indirect. Here we identify an sRNA, Pxr, that negatively regulates fruiting body development in *Myxococcus xanthus*. We further show that a spontaneous evolutionary mutation in Pxr abolished its regulatory function and thereby adaptively restored developmental proficiency to a socially defective cheater. In wild-type *M. xanthus*, development is initiated only upon starvation, but deletion of *pxr* allows development to proceed at high nutrient levels. Thus, Pxr serves as a major checkpoint controlling the transition from growth to development in the myxobacteria. These findings show that an sRNA molecule governs a complex form of multicellular development in prokaryotes and directly demonstrate the ability of sRNA regulators to facilitate evolutionary adaptations of major phenotypic effect.

Materials and Methods

M. xanthus strains were grown in CTT liquid medium (in which casitone provides carbon and amino acids essential for growth, (*1*)) at 32°C, 300 rpm or on CTT 1.5% agar plates and development assays were performed on TPM agar plates (identical to CTT agar except lacking casitone) as described previously (*2, 3*) or on TPM supplemented with casitone (Fig. 1). The images in Fig. 1D were taken four days after cultures were spotted onto their respective treatments and sporulation data was collected after six days. Competent *Escherichia coli* DH5α (*4*) and TOP10 (Invitrogen) cells were used for plasmid cloning and were grown at 37°C in Luria-Bertani broth (LB) (*5*) or on LB 1.5% agar plates supplemented with appropriate antibiotics (ampicillin and kanamycin at 100 and 40 *ug*/ml, respectively).

Total RNA was extracted from vegetative cultures growing in CTT liquid or developmental cultures starving on TPM agar and small RNA fragments were enriched with the MirVana miRNA isolation kit (Ambion). RNA concentration was determined with a Nanodrop spectrophotometer. Equal amounts of RNA were electrophoresed in 10% SequaGel (National Diagnostics) and electro-transferred onto a BrightStar®-Plus positively charged nylon membrane (Ambion). After UV cross-linking, the membrane was pre-hybridized in 5 ml UltraHyb-Oligo buffer for 30 min. and then hybridized in the same solution containing 100 pmol 3'Biotin-TEG-*pxr* oligo probe (Sigma) overnight. Pxr RNA was detected with BrightStar® Biodetect non-isotopic kit (Ambion). Prediction of Pxr secondary structure was performed with Mfold (*6*).

Plasmid construction

To construct pCR_1079, a promoter-less internal DNA fragment of Mxan_1079 was amplified with the forward and reverse primers GTCTTTGCCCGGCTGTTTC and

CCCGCTTCACGTTGCGGAC , respectively and then cloned into pCR_Blunt (Invitrogen). Construction of the marker-less allele-exchange plasmid pBJ_Δ*pxr* involved a two-step cloning procedure (*7*). In the first step, a DNA fragment preceding the putative *pxr* gene was PCR amplified with the primers GV372 (CTCTGGCGGAAGATGAAGCGGC) and GV490 (CCTTTCGTCGCGAGCCGATGTGTCCCGCGCATTCC) and a second DNA fragment following the *pxr* gene with the primers GV489 (TCGGCTCGCGACGAAAGGAA) and GV370 (GCCAGCTTGCCGGGAATC). A subsequent PCR reaction was used to fuse the two PCR products by overlapping extension with the complementary18-nt sequences underlined in both GV489 and GV490 and to amplify the fused fragment with GV370 and GV372. The resulting PCR fragment was cloned into pCR-Blunt to make pCR_Δ*pxr*, which is lacking 128 bp of the *pxr* gene. For the second cloning step, the PCR insert of pCR_Δ*pxr* was excised with BamHI and EcoRV double digest and re-ligated into the BamHI-HincII linearized pBJ113 vector (*7, 8*) to make the final plasmid pBJ_Δ*pxr*. The parental plasmid pBJ113 carries a kanamycin-resistance gene and *galK*, causing galactose sensitivity in *M. xanthus.*

The plasmids pGVTu_pxr^{+} and pGVTu_pxr^{PX} contain and express (from the *pxr* promoter) the DK1622/GJV1 *pxr* allele (pxr^{+}) and the PX (GJV81) *pxr* allele (pxr^{PX}), respectively. These plasmids also contain a kanamycin-resistance marker gene and the *M. xanthus* phage Mx8 *att* site that allows integration into the *M. xanthus* genome (*9*). The predicted *pxr* coding region was PCR-amplified from GJV1and GJV81 with primers GV491 (TTGGATCCGAAATGGACGGGTTCATAG) and GV492 (TTAAGCTTTCGTVGVGAGCCGAG). GV491 is tailored with the BamHI restriction site and GJV492 with the HindIII site (underlined). The PCR product was digested with BamHI and

HindIII and cloned into pGVTu1 after linearization with the same enzymes. Further details of plasmid construction are available upon request.

M. xanthus strain nomenclature and construction

The generation of *M. xanthus* strains GJV201 (here also "OC", Table S1) and GJV202 (here also PX) was described previously (*2*), where they were referred to as GVB207.3/PX- and GVB207.3/PX+, respectively. For simplicity, we here use the common core descriptor of 'OC' for strains GVB207.3, GJV32 (the original "OC" (*2*)) and GJV201 because these strains share the same developmental defect and are identical except that GJV32 is marked with a chromosomally integrated plasmid bearing a kanamycin-resistance gene. Similarly, we use the core descriptor 'PX' for strains GJV81 (the original "PX") and GJV202 because these strains share the PX positive developmental phenotype and also differ only in the presence/absence of a plasmid bearing a kanamycin-resistance gene. We distinguish between the OC and PX variants as necessary with their "GJV" numerical designation. GJV81 (PX) originally evolved directly from GJV32 (*2*) and therefore carries the same resistance marker. GJV202 was generated by markerless exchange of the pxr^{PX} allele for the ancestral pxr^{+} allele in GJV207.3 after integration and excision of plasmid pNY-PX.2. GJV201 was also derived from integration and excision of plasmid pNY-PX.2 in GJV207.3, except that the original pxr^{+} was not replaced, thus restoring the intermediate integrant to the original GVB207.3 genotype. GJV203, GJV204, GJV208 and GJV209 were generated by plasmid integration into a genomic background of interest (see Table S1) after electroporation of competent cells. GJV205 was generated by double-crossover replacement of the GJV202 chromosomal region containing the pxr^{PX} allele and Mxan_1079 (pxr^{PX}/$mxan1079^{+}$) with the corresponding region in GJV203 containing both pxr^{+} allele and the

disrupted mutant allele of Mxan_1079 (*pxr*$^{+}$/*mxan1079*). This homologous exchange was accomplished by electroporation of GJV202 with fragmented chromosomal DNA of GJV203, subsequent selection for kanamycin-resistant transformants and *pxr*$^{+}$ genotype confirmation by sequencing. Strains GJV206 and GJV207 were generated by replacement of the native *pxr*$^{+}$ allele with a markerless in-frame deletion of *pxr* in strains GJV1 and GVB207.3, respectively, by a counter-selection method described previously (*7, 10*).

Supplementary Online Text

The discovery of non-coding sRNA regulatory elements has transformed our understanding of gene regulation and its evolution in all domains of life (*11-14*). In bacteria, sRNAs regulate a wide range of functions, including social traits such as quorum sensing and biofilm formation (*15-19*). Previous inferences regarding the role of sRNA elements in adaptive evolution have been made indirectly from the comparative analysis of extant natural variation (*20, 21*). Alternatively, molecular analysis of adaptations occurring in experimental populations may provide direct and novel insights into how adaptive evolution occurs via modification of sRNA molecules and their associated regulatory pathways. Here we document how analysis of a spontaneous adaptive mutation in a social microbe has revealed a new category of sRNA regulator and how deactivation of this regulator mediates the adaptive restoration of a previously defective social trait. These findings exemplify how characterizations of mutations in experimentally evolved organisms can shed light not only on the genetic basis of adaptation but also on the fundamental biology of model organisms.

Many species of myxobacteria (Gram- delta-proteobacteria, order Myxococcales), including the model species *Myxococcus xanthus,* form multicellular fruiting bodies in response to starvation through a developmental process that requires several intercellular signals and social

coordination of cell movement (*22-24*). Many myxobacteria are also predators of other microbes and require amino acids normally derived from prey or organic detritus for vegetative growth (*25*). Depletion of amino acids triggers the initiation of fruiting body development in high density populations (*26*), which involves the aggregation of cells into fruiting body structures and the differentiation of vegetative cells into stress-resistant spores.

The developmentally defective strain OC (here referring jointly to the nearly identical strains GVB207.3, GJV32 and GJV201) is a 1000th-generation descendant of the developmentally proficient "wild-type" strain GJV1 (a derivative of DK1622 (*3, 27*), Table S1). The genome sequence of OC differs from that of GJV1 by 14 mutations that accumulated during a laboratory evolution experiment (*27*). OC is a developmental cheater that can exploit GJV1 in chimeric groups to produce spores more efficiently than GJV1 despite OC having a severe developmental defect in pure culture. Strain PX evolved from the defective cheater OC during a laboratory competition experiment between OC and a marked variant of GJV1 in which OC caused a population crash upon reaching high frequency due to its developmental defect (*2*). PX emerged from this crash as the dominant competitor during development.

The single mutation conferring the PX phenotype was identified by sequencing the PX genome (*27*) and genetic transfer of the mutation into the OC genome (*2*). The mutation was found to lie between predicted coding sequences for the σ^{54}-dependent DNA-binding response regulator Nla19 (*28*) (Mxan_1078) and an annotated GCN5-related N-acetyltransferase (Mxan_1079) (*29*) (Fig. S1A). The mutation in PX is a C→A substitution located 128 bp upstream of *Mxan_1079 that up-r*egulates transcription of this gene during development in strain PX relative to GJV1 and OC (*30*).

The C→A mutation in PX was found to lie within the first of three predicted hairpin loops in the *pxr* region (Fig. S1B). Loop sequences are known to be required for the function of several sRNAs in *E. coli (31).* Polymorphisms in *pxr* between *S. aurantiaca* and *M. xanthus* (Fig. S1B) occur within predicted bulges or loops except for the C/U polymorphism on the left-side of the third stem and the G/A polymorphism on the opposite side of the same stem, which are complementary changes that retain the stem-loop structure. BLAST analysis failed to detect any *pxr* homolog in sequenced myxobacteria species other than in *S. aurantiaca,* specifically *Sorangium cellulosum (32)* and *Anaeromyxobacter dehalogenans (33),* thus suggesting a recent origin of the Pxr regulatory system within the Myxococcales sub-clade shared by *M. xanthus and S. aurantiaca (34).*

The GC ratios of Mxan_1078 and Mxan_1079 are 71% and 70%, respectively, similar to the overall ratio of 69% GC across the entire *M. xathus* genome (*29*). However, the 413 bp region between Mxan_1078 and Mxan_1079 that includes *pxr* is only 57% GC, suggesting either that this region has been recently acquired horizontally and/or is under selective constraint.

The hypothesis that Pxr-S is the active Pxr negative regulator of development (rather than Pxr-L) is supported not only by the data presented in Fig. 1B and Fig. S3, but also by the fact that a transposon-insertion mutant of the unmarked OC variant GVB207.3 exhibits a developmentally proficient, PX-like phenotype and produces Pxr-L but not Pxr-S (data not shown).

Prokaryotes utilize the RelA-SpoT-homolog stringent response to regulate changes in gene expression upon starvation (*35*). Nutrient depletion triggers synthesis of guanosine-5'-diphosphate-3'-diphosphate (ppGpp) and guanosine-5'-triphosphate-3'-diphosphate (pppGpp) (together (p)ppGpp) by RelA homologs. High levels of accumulated (p)ppGpp then trigger

genome-wide changes in gene expression that inhibit growth functions and induce stress functions. Myxobacterial development is initiated by a regulatory connection between the stringent response and a unique quorum-sensing system. High levels of (p)ppGpp generated by the stringent response induce A-signaling, which involves hydrolysis of cell-surface proteins to generate an extra-cellular pool of amino acids that serve as a quorum signal to initiate cell aggregation and trigger development-specific changes in gene expression (*26, 36*).

Strain OC does not appear to be defective at the stringent response. Two genes, *sdeK* and *csgA*, that are up-regulated by high (p)ppGpp levels in wild-type *M. xanthus* show wild-type expression patterns in OC (*30*). In contrast, the *fruA* gene is up-regulated in response to the A-signal in wild-type but not in OC (*30*). However, the Pxr-debilitating C→A mutation in strain PX restores development-specific expression of *fruA* (*30*). These findings suggest that *pxr* may prevent the initiation of A-signaling in the absence of the stringent response and that (p)ppGpp accumulation triggers the development-specific reduction in Pxr-S.

Previous studies have shown that mutations in the *mcp3B* gene of the Che3 cluster (*37*), *socE* (*38*) and *nsd* (*39*) cause limited degrees of developmental progression at high nutrient levels. However, despite their partial developmental phenotypes, none of these mutants produce a high number of viable spores in the presence of abundant nutrients. In stark contrast, the *pxr* mutant not only produces many viable spores over a range of high nutrient concentrations at which GJV1 does not, but does so at levels similar to GJV1 when the latter is completely starved (Fig. 1B). The discovery of *pxr* not only reveals the most potent negative regulator of myxobacterial developmental found to date, but will likely also lead to the identification of additional novel genes involved in the transition from vegetative growth to multicellular development.

Understanding the relative contributions of changes in the amino acid sequences of proteins vs. changes in non-protein regulatory elements to the evolution of morphological diversity is a major goal of "evo-devo" studies (*40*). Small RNA elements regulate large-scale changes in genome-wide expression profiles and are therefore prime candidates in the search for loci that have played major roles in the morphological diversification of life. Here we have shown that the novel sRNA Pxr plays a central role in regulating the complex process of myxobacterial fruiting body development and that a spontaneous mutation in this regulator mediated the adaptive restoration of *M. xanthus* social development.

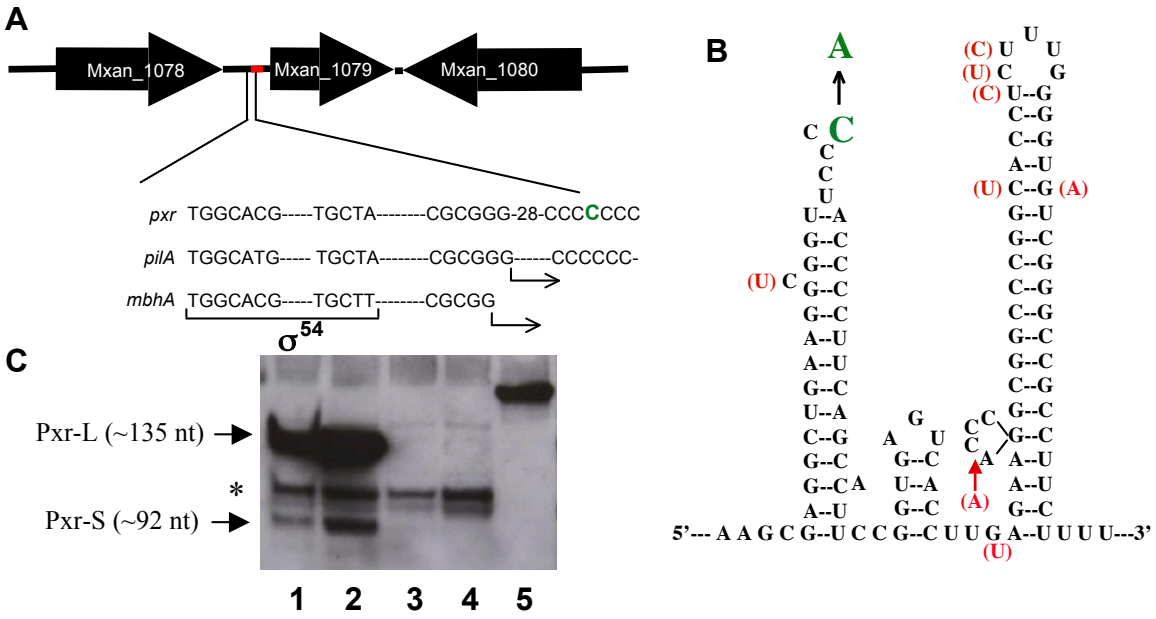

Figure S1. Evidence of a non-coding small RNA between Mxan_1078 and Mxan_1079. (A) The *pxr* region, including a predicted σ^{54} promoter sequence highly similar to the *M. xanthus pilA* (*41*) and *mbhA* (*42*) σ^{54} promoters. Dash marks represent individual nucleotides (except those flanking "28" for the *pxr* promoter region sequence, which represents 28 nucleotides between the adjacent sequences). The green C indicates the position of the C→A mutation in strain PX (also in (B)). Arrows below the *pilA* and *mbhA* promoter region sequences indicate known transcription start sites. The red bar represents the position of the sequence depicted in (B). (B) The predicted structure of Pxr RNA, which has a predicted formation energy of -58 kcal/mol. Base symbols in parentheses indicate polymorphisms between *M. xanthus* and *Stigmatella aurantiaca*. (C) A Northern blot showing the presence of long and short forms of Pxr RNA (Pxr-L and Pxr-S, respectively) produced by GJV1 (lane 1) and OC (GJV201, lane 2) but not by OC Δ*pxr* (GJV207, two independent deletion mutants shown in lanes 3 & 4). Lane 5 shows a 150 nt Watson–strand fragment derived from PCR of the *pxr* region that served as positive control for the oligo probe. The asterisk marks bands generated by binding of the probe to non-Pxr RNA. Pxr-L and Pxr-S sizes were estimated by comparing band mobility to the Ambion RNA Century™-Plus size marker.

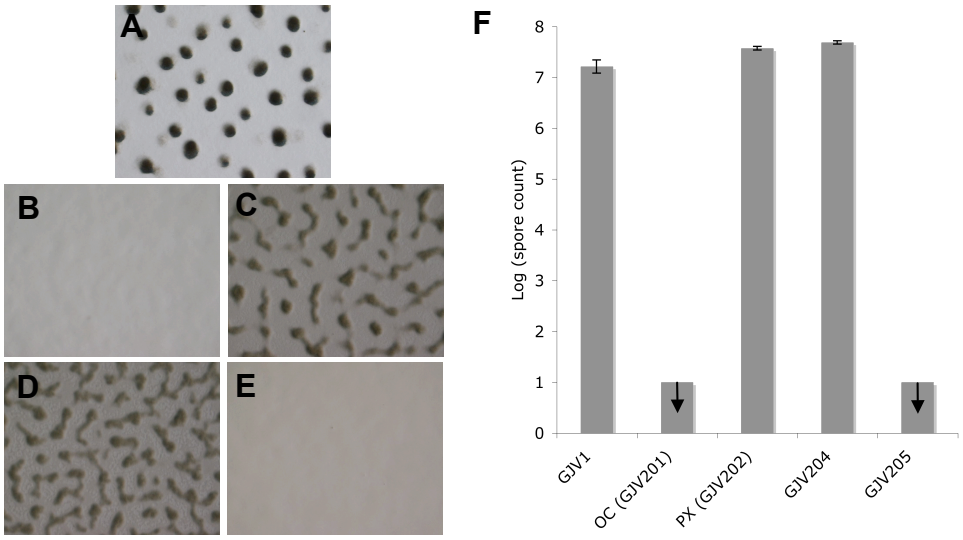

Figure S2. The PX phenotype is independent of Mxan_1079. Developmental phenotypes (120 h) of (A) GJV1, (B) OC (GJV201), (C) PX (GJV202), (D) GJV204 and (E) GJV205. (F) Spore production of the five strains shown in A-E. Arrows indicate that no spores were produced at the lower limit of detection.

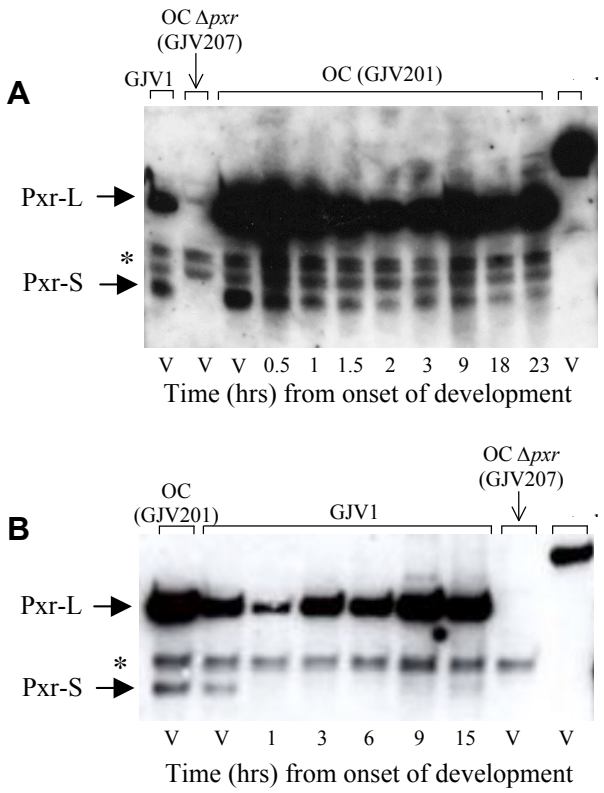

Figure S3. (A) Pxr-L and Pxr-S accumulation remains high in the fruiting-defective strain OC (GJV201) throughout 24 h of starvation. The final lane shows a 150 nt *pxr* positive control (see Fig. S1C legend). "V" refers to vegetatively growing cells harvested immediately prior to the initiation of starvation. (B) Accumulation of Pxr-S is greatly reduced or eliminated shortly after the onset of starvation in the developmentally proficient wild-type GJV1. The asterisk marks bands generated by binding of the probe to non-Pxr RNA.

Table S1. Strains and plasmids.

Strains/plasmids	**Description**	**Ref./source**
GJV1	Derivative isolate of DK1622, *pxr*$^{+}$ (wild-type allele of *pxr*)	(*2, 29*)
GVB207.3	Evolutionary descendant of GJV1(*3, 43*), *pxr*$^{+}$ (here also "OC")	(*2, 3*)
GJV32	GVB207.3 kan^{R} ("OC" in ref. (*2*))	(*2*), (*43*)
GJV81	Descendant of GJV32, *pxr*^{PX} (C→A substitution allele of *pxr*), kan^{R} ("PX" in ref. (*2*))	(*2*)
GJV201	GVB207.3 *pxr*$^{+}$ after excision of suicide plasmid$^{(2)}$ ("GVB207.3/PX-" in ref. (*2*), here also "OC")	(*2*)
GJV202	GVB207.3 *pxr*^{PX} after excision of suicide plasmid$^{(2)}$ ("GVB207.3/PX+" in ref. (*2*), here also "PX")	(*2*)
GJV203	GJV1 *pxr*$^{+}$ *mxan1079::pCR_1079*, kan^{R}	This study
GJV204	GJV202 *pxr*^{PX} *mxan1079::pCR_1079*, kan^{R}	This study
GJV205	GJV202 *pxr*$^{+}$ *mxan1079::pCR_1079*, kan^{R}	This study
GJV206	GJV1 Δ*pxr*	This study
GJV207	GVB207.3 Δ*pxr*	This study
GJV208	GJV207 *att*::*pGVTu_pxr*$^{+}$, kan^{R}	This study
GJV209	GJV207 *att*::*pGVTu_pxr*^{PX}, kan^{R}	This study
pCR-Blunt	Cloning vector	Invitrogen
pCR_1079	pCR-Blunt with *Mxan_1079* fragment insert	This study
pBJ113	Allele exchange plasmid with kan^{R} and *galK* genes	(*7*)
pCR_Δ*pxr*	pCR-Blunt with Mxan_1078-Mxan_1079 intergenic region missing a 128 bp *pxr* fragment	This study
pBJ_Δ*pxr*	pBJ113 with Mxan_1078-Mxan_1079 intergenic region missing a 128 bp *pxr* fragment	This study
pGVTu1	2.3 kb Mx8att site, kan^{R}	
pGVTu_*pxr*$^{+}$	pGVTu1 *pxr*$^{+}$, kan^{R}	This study
pGVTu_*pxr*^{PX}	pGVTu1 *pxr*^{PX}, kan^{R}	This study

References

1. J. Hodgkin, D. Kaiser, *Proc. Natl Acad. Sci. USA* **74**, 2938 (1977).
2. F. Fiegna, Y. T. N. Yu, S. V. Kadam, G. J. Velicer, *Nature* **441**, 310 (2006).
3. G. J. Velicer, L. Kroos, R. E. Lenski, *Proc. Natl Acad. Sci. USA* **95**, 12376 (1998).
4. D. Hanahan, *J Mol Biol* **166**, 557 (1983).
5. J. Sambrook, E. F. Fritsch, J. Sambrook. (Cold Spring Harbor Laboratory, Cold Spring Harbor, N.Y., 1989).
6. M. Zuker, *Nucleic Acids Research* **31**, 3406 (2003).
7. A. M. Rodriguez, A. M. Spormann, *J. Bacteriol.* **181**, 4381 (1999).
8. Z. Yang, Y. Geng, D. Xu, H. B. Kaplan, W. Shi, *Mol Microbiol* **30**, 1123 (1998).
9. V. Magrini, C. Creighton, P. Youderian, *J. Bacteriol.* **181**, 4050 (1999).
10. T. Ueki, S. Inouye, M. Inouye, *Gene* **183**, 153 (1996).
11. G. Stefani, F. J. Slack, *Nat. Rev. Mol. Cell Biol.* **9**, 219 (2008).
12. M. J. Axtell, J. L. Bowman, *Trends Plant. Sci.* **13**, 343 (2008).
13. J. Lu *et al.*, *Mol. Biol. Evol.* **25**, 929 (2008).
14. R. Niwa, F. J. Slack, *Curr. Opin. Genet. Dev.* **17**, 145 (2007).
15. S. Gottesman, *Trends Genet.* **21**, 399 (2005).
16. K. Heurlier *et al.*, *J. Bacteriol.* **186**, 2936 (2004).
17. D. H. Lenz *et al.*, *Cell* **118**, 69 (2004).
18. M. Bejerano-Sagie, K. B. Xavier, *Curr. Opin. Microbiol.* **10**, 189 (2007).
19. L. S. Waters, G. Storz, *Cell* **136**, 615 (2009).
20. E. J. Chapman, J. C. Carrington, *Nat. Rev. Genet.* **8**, 884 (2007).
21. H. Quach *et al.*, *Am. J. Hum. Genet.* **84**, 316 (2009).
22. D. R. Zusman, A. E. Scott, Z. Yang, J. R. Kirby, *Nat. Rev. Microbiol.* **5**, 862 (2007).
23. L. Kroos, *Annu. Rev. Gen.* **41**, 13 (2007).
24. D. Kaiser, *Annu. Rev. Microbiol.* **58**, 75 (2004).
25. J. E. Berleman, J. R. Kirby, *FEMS Microbiol. Rev.* **33**, 942 (2009).
26. H. B. Kaplan, L. Plamann, *FEMS Microbiol. Lett.* **139**, 89 (1996).
27. G. J. Velicer *et al.*, *Proc. Natl Acad. Sci. USA* **103**, 8107 (2006).
28. N. B. Caberoy, R. D. Welch, J. S. Jakobsen, S. C. Slater, A. G. Garza, *J. Bacteriol.* **185**, 6083 (2003).
29. B. S. Goldman *et al.*, *Proc. Natl Acad. Sci. USA* **103**, 15200 (2006).
30. S. V. Kadam, S. Wegener-Feldbrugge, L. Sogaard-Andersen, G. J. Velicer, *Mol. Biol. Evol.* **25**, 1274 (2008).
31. S. Gottesman, *Annu. Rev. Microbiol.* **58**, 303 (2004).
32. S. Schneiker *et al.*, *Nat. Biotechnol.* **25**, 1281 (2007).
33. S. H. Thomas *et al.*, *PLoS ONE* **3**, e2103 (2008).
34. C. Sproer, H. Reichenbach, E. Stackebrandt, *Int. J. Syst. Bacteriol.* **49**, 1255 (1999).
35. K. Potrykus, M. Cashel, *Annu. Rev. Microbiol.* **62**, 35 (2008).
36. B. Z. Harris, D. Kaiser, M. Singer, *Genes Dev.* **12**, 1022 (1998).
37. J. R. Kirby, D. R. Zusman, *Proc. Natl Acad. Sci. USA* **100**, 2008 (2003).
38. E. W. Crawford, Jr., L. J. Shimkets, *Mol. Microbiol.* **37**, 788 (2000).
39. M. Brenner, A. G. Garza, M. Singer, *J. Bacteriol.* **186**, 3461 (2004).
40. S. B. Carroll, *Cell* **101**, 577 (2000).

41. S. S. Wu, D. Kaiser, *J. Bacteriol.* **179**, 7748 (1997).
42. J. M. Romeo, D. R. Zusman, *J. Bacteriol.* **173**, 2969 (1991).
43. G. J. Velicer, R. E. Lenski, L. Kroos, *J. Bacteriol.* **184**, 2719 (2002).